Discover Nano

Discover

Research

Scalable synthesis of $BiVO_4$ thin films via anodic plating and thermal calcination

Haoyang Jiang[1] · Yongcheng Xiao[1] · Miao Zhong[1]

Received: 17 December 2022 / Accepted: 17 January 2023

Abstract
Fabrication of high-quality semiconductor thin films has long been a subject of keen interest in the photocatalytic field. Here, we report a facile, solution-based anodic plating and calcination for large-scale synthesis of $BiVO_4$ thin films on indium tin oxide coated glass for use as photoanodes in solar water splitting. Using Na_2SO_3 as a sacrificial reagent, continuous solar H_2 production with 94% Faradaic efficiency was obtained over 6 h of photoelectrochemical water splitting.

Keywords Anodic plating · Thin film · Bismutite · Bismuth vanadate · Solar hydrogen generation

Abbreviations

ITO	Indium tin oxide
PEC	Solar-driven photoelectrochemical
SEM	Scanning electron microscopy
XPS	X-ray photoelectron spectroscopy
XRD	X-ray diffraction
TGA	Thermogravimetric analysis

Introduction

Solar-driven photoelectrochemical (PEC) water splitting is a promising route for the large-scale production of renewable hydrogen fuel from water [1–5]. In the past decades, much effort has been made to improve the overall energy efficiency of PEC devices [6–9]. In terms of the photocathodes, high photocurrent densities with low overpotentials have been realized using *p*-type solar-cell materials in combination with hydrogen-evolution co-catalysts. However, the improvement in photoanodes remains limited [10].

Among a range of photoanodic materials, $BiVO_4$ has attracted research attention because it has a deep valance band position for the oxygen evolution reaction [11]. Also, $BiVO_4$ is relatively stable in neutral aqueous environments (pH

Supplementary Information The online version contains supplementary material available at https://doi.org/10.1186/s11671-023-03774-z.

✉ Miao Zhong, miaozhong@nju.edu.cn | [1]College of Engineering and Applied Sciences, Nanjing University, 163 Xianlin Avenue, Qixia District, Nanjing 210023, China.

7–9) [12, 13]. Over 100-h PEC water oxidation has been reported using crystalline $BiVO_4$ photoanodes [14]. One of the remaining challenges for $BiVO_4$ is to increase the photocurrent density under photocatalytic conditions without applying any external electrical potential. To this end, Choi et al. reported the synthesis of nanoporous $BiVO_4$ photoanodes in a two-step process using BiOI nanoplates as the precursor [15]. Nanostructure certainly improves the charge separation; however, it also presents a difficulty for fabricating a *p-n* junction that is able to cover the entire $BiVO_4$ to make stand-alone, photocatalytic water-splitting catalysts.

In this work, we report a facile synthesis of $BiVO_4$ thin films on transparent, conductive indium tin oxide (ITO) substrates using anodic plating and thermal calcination. A homogeneous mixture of the anodically deposited bismutite hydrate ($(BiO)_4(OH)_2CO_3$) and vanadium ions (Fig. S1 in the supporting information) allows nucleation of stichometrical $BiVO_4$ during calcination. Also, bismutite hydrate decomposes at temperatures > 500 °C and releases CO_2; the synthesized $BiVO_4$ is thus free of contamination. Using Na_2SO_3 as a sacrificial reagent, stable photoelectrochemical H_2 generation was realized over 6 h of water splitting. The present study shows a promising solution-based process for the preparation of $BiVO_4$ thin films for use in water-splitting applications.

Results and discussion

Layer-structured bismutite and its hydrate were first reported in 1943 [16] and systematically studied in 1984 [17]. In mineralogy, bismutite is a well-established solid carbonate in the system Bi_2O_3-CO_2-H_2O [16] with a natural color of yellow to brown. In the laboratory, the synthesis of bismutite has only been reported using the hydrothermal method and with the products in the form of particles [17, 18]. In the present study, we found that anodic plating can also synthesize amorphous $Bi_4O_4(OH)_2CO_3$ thin films on ITO glass via Kolbe electrolysis with the presence of Bi ions, following the Eq. 1:

$$CH_3COONa + Bi(NO_3)_3 + H_2O \overset{+2.3V_{Ag/AgCl}}{\longrightarrow} (BiO)_4(OH)_2CO_3 + NaNO_3 \tag{1}$$

Figure 1 shows the anodic plating of amorphous $Bi_4O_4(OH)_2CO_3$ films on ITO substrates using NaCOOH and $Bi(NO_3)_3$ solutions at pH ~ 5. The applied potential is + 2.3 V vs Ag/AgCl ($V_{Ag/AgCl}$). After 7-min anodic plating, ~ 300-nm-thick film was plated. Likely, the NaCOOH was oxidized at anodic potentials (Eq. 1) to form CO_2 on the electrode surfaces. With the presence of Bi^{3+} in the solution, $Bi_4O_4(OH)_2CO_3$ precipitated on the electrodes. We also found that Bi metals precipitated on the cathode. This is because the reduction potential of Bi^{3+} to Bi was + 0.2 V_{RHE}, which is more positive than 0 V_{RHE} of the hydrogen evolution reaction. To suppress the Bi precipitation, *p*-benzoquinone can be added to the electrolyte. The cathodic reaction then mainly shifts to the reduction of *p*-benzoquinone to 1,4-hydroquinone with a reduction potential of ~ + 0.6 V_{RHE} (Fig. S2). The optical images of the anodically plated amorphous $Bi_4O_4(OH)_2CO_3$ films are provided on the right panel in Fig. 1, which shows the change of color at the different time of the plating.

To understand anodic plating details, $Bi_4O_4(OH)_2CO_3$ films were characterized by scanning electron microscopy (SEM), X-ray photoelectron spectroscopy (XPS), X-ray diffraction (XRD), UV–Vis diffuse-reflectance analyses and thermogravimetric analysis (TGA) (Figs. 2, 3 and Figs. S3, S4 in the supporting information). To evaluate constituent compositions, the plated $Bi_4O_4(OH)_2CO_3$ films were scratched from ITO/glasses for TGA with a temperature rise from 30 to 500 °C in an N_2

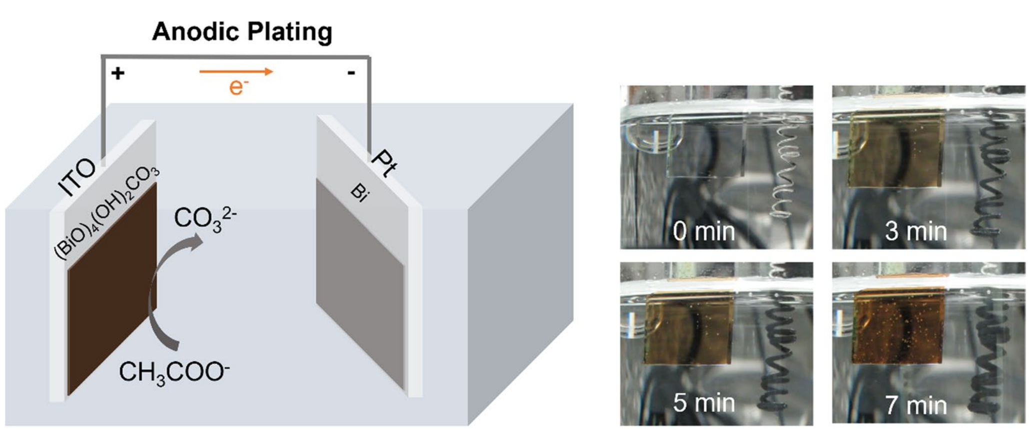

Fig. 1 Schematic of the anodic plating for depositing $(BiO)_4(OH)_2CO_3$ films on ITO glasses

atmosphere (N_2 was used to avoid adsorption of CO_2 from the air). As shown in Fig. 2a, three steps of endothermic decomposition were obtained in a TGA run for $Bi_4O_4(OH)_2CO_3$. A continuous weight loss of 5.6% below 180 °C was observed, likely attributed to absorbed solvent and water [17]. $Bi_4O_4(OH)_2CO_3$ decomposition often occurs in two stages [17]: major loss of hydrate with a small loss of carbon dioxide at 180–240 °C and major loss of carbon dioxide at 240–500 °C. The calculation of weight losses in each step yielded an empirical formulation of $(BiO)_4(OH)_{1.01}(CO_3)_{0.94}$ of the anodically plated films, which agreed with the predicted products of $Bi_4O_4(OH)_2CO_3$. As a reference, we also analyzed $Bi_2O_2CO_3$ powder (Wako, 99.5%) by TGA under the same conditions. Decomposition to release carbon dioxide was observed at 240–500 °C with a weight loss of 9.6 wt%, close to the theoretic value of 8.6 wt%. A slight shift of decomposition onset temperature of $Bi_2O_2CO_3$ compared to that of plated $Bi_4O_4(OH)_2CO_3$ films was likely due to the crystalline and amorphous nature of the two materials. This result suggested that amorphous $Bi_4O_4(OH)_2CO_3$ films were anodically plated on ITO.

Figure 3a shows the optical images of the synthesis process of $BiVO_4$ thin films on ITO substrates. In brief, we deposited amorphous Bi precursors on ITO substrates and calcinated them with the vanadium source at 520 °C. After the reaction, we washed the surface residual vanadium chemicals using 1 M NaOH solution. This process was similar to our previous report, in which the $BiVO_4$ was fabricated via three steps: precursor deposition, pre-calcination of the deposited films in the air at 200 °C, and calcination with a vanadium source at 490–530 °C. We used two-step fabrication, which was able to fabricate $BiVO_4$ thin films with similar morphology. The Bi precursor materials were calcined in the air at 520 °C (Fig. 3c) for 2 h. The fabricated $BiVO_4$ films were in a monoclinic structure, which agreed with the previous report [8].

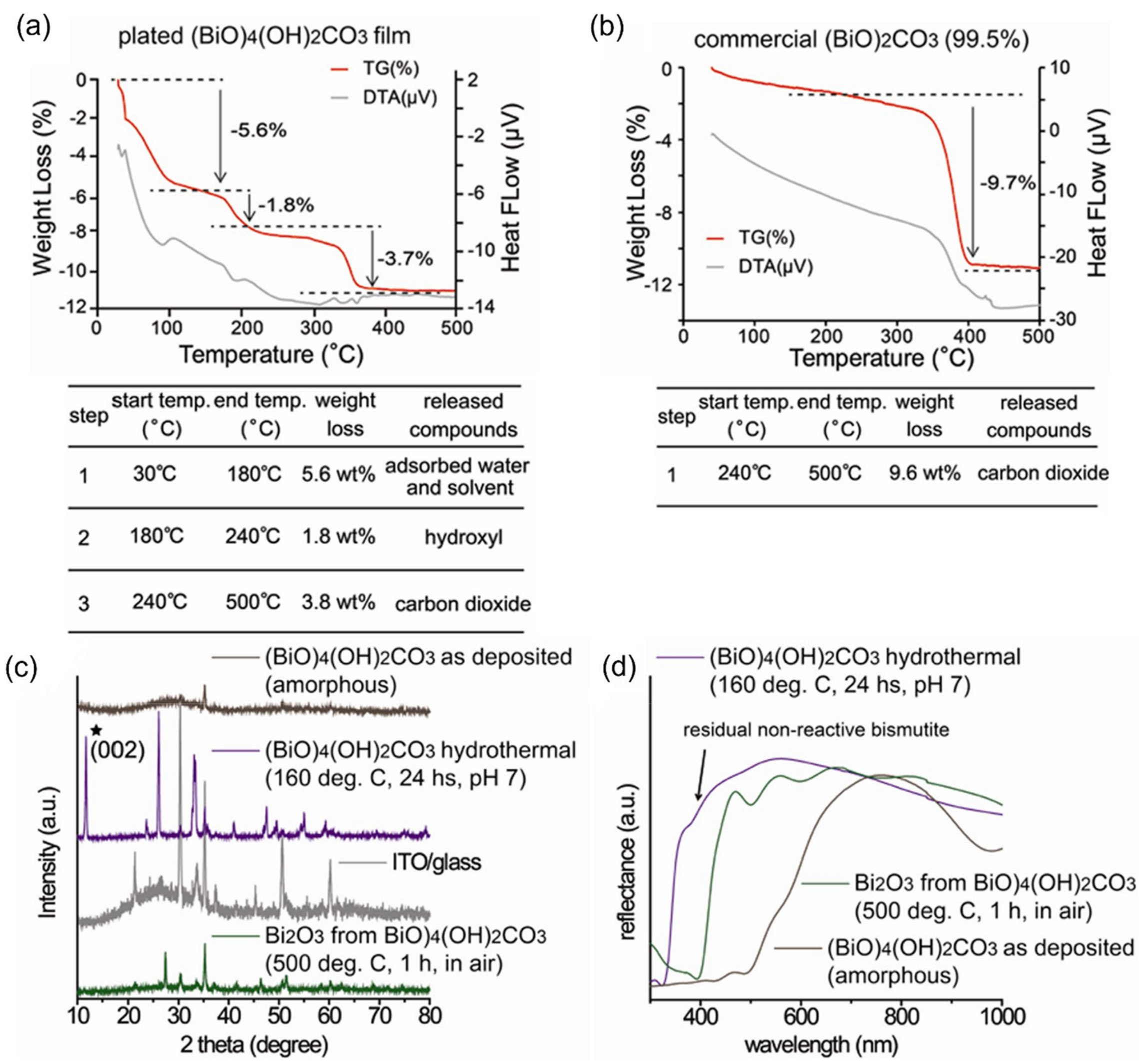

step	start temp. (°C)	end temp. (°C)	weight loss	released compounds
1	30℃	180℃	5.6 wt%	adsorbed water and solvent
2	180℃	240℃	1.8 wt%	hydroxyl
3	240℃	500℃	3.8 wt%	carbon dioxide

step	start temp. (°C)	end temp. (°C)	weight loss	released compounds
1	240℃	500℃	9.6 wt%	carbon dioxide

Fig. 2 **a** TG and DTA of a plated $(BiO)_4(OH)_2CO_3$ film. **b** TG and DTA of the commercial $(BiO)_2CO_3$ (99.5%). **c** XRD pattern of the as-plated $(BiO)_4(OH)_2CO_3$, hydrothermal-treated $(BiO)_4(OH)_2CO_3$, ITO and Bi_2O_3 calcinated from $(BiO)_4(OH)_2CO_3$. **d** UV–vis diffuse reflectance spectra of the as-plated $(BiO)_4(OH)_2CO_3$, hydrothermal-treated $(BiO)_4(OH)_2CO_3$, ITO and Bi_2O_3 calcinated from $(BiO)_4(OH)_2CO_3$

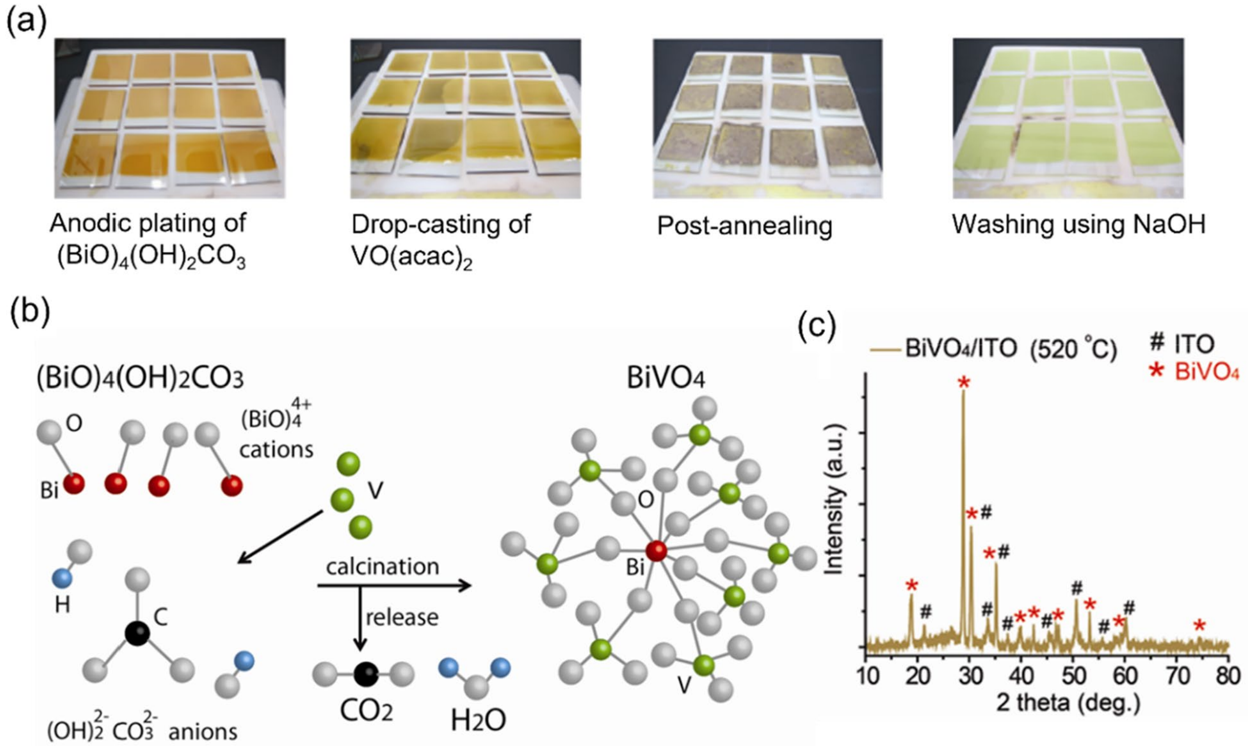

Fig. 3 **a** Optical images of the solution-based process for the synthesis of $BiVO_4$ films on ITO glass (12 pieces of the 2 cm × 2 cm samples). **b** Schematic diagram of a proposed reaction mechanism. **c** XRD patterns of the $BiVO_4$/ITO synthesized at 520 °C

The scanning electron microscopy (SEM) images of the plated $Bi_4O_4(OH)_2CO_3$ film are present in Fig. S3 in the supporting information. The 7-min anodically plated amorphous $Bi_4O_4(OH)_2CO_3$ film was ~ 300 nm thick on the ITO substrate (Fig. S3). Bi was detected on the surface and in the bulk of the film (Fig. S4). As shown in cross-sectional SEM images in Fig. 4, the $BiVO_4$ film was made of large $BiVO_4$ particles with an in-plane diameter of ~ 500–1000 nm and a thickness of ~ 300 nm. Such large $BiVO_4$ crystalline likely decreased the number of boundaries between particles. Therefore, improved photoelectrochemical performance was realized.

Finally, we tested the photoelectrochemical performance of the fabricated $BiVO_4$ films in 0.1 M Na_2SO_3 solution. As shown in Fig. 5a, a quick raise of the photocurrent density was observed with $BiVO_4$ films with the increase of the positive potential. At 0.9–1.2 V_{RHE}, the photocurrent density reached a plateau of ~ 5 mA/cm^2 under simulated solar light irradiation. We used a micro gas chromatography (micro-GC) to analyze the hydrogen evolution, which was stable over 6-h photoelectrochemical water splitting at 0.9 V_{RHE} (Fig. 5b).

Conclusions

In this work, anodic plating was reported for the fabrication of Bi precursors on the indium tin oxide (ITO) substrates. Following high-temperature calcination with vanadium sources, crystalline $BiVO_4$ was fabricated on ITO substrates. The photocurrent density reached ~ 4–5 mA/cm^2 at 0.9–1.2 V_{RHE} in Na_2SO_3-containing electrolytes under simulated solar illumination. The developed electrochemical deposition and thermal calcination may offer a new pathway for the synthesis of photocatalytic materials.

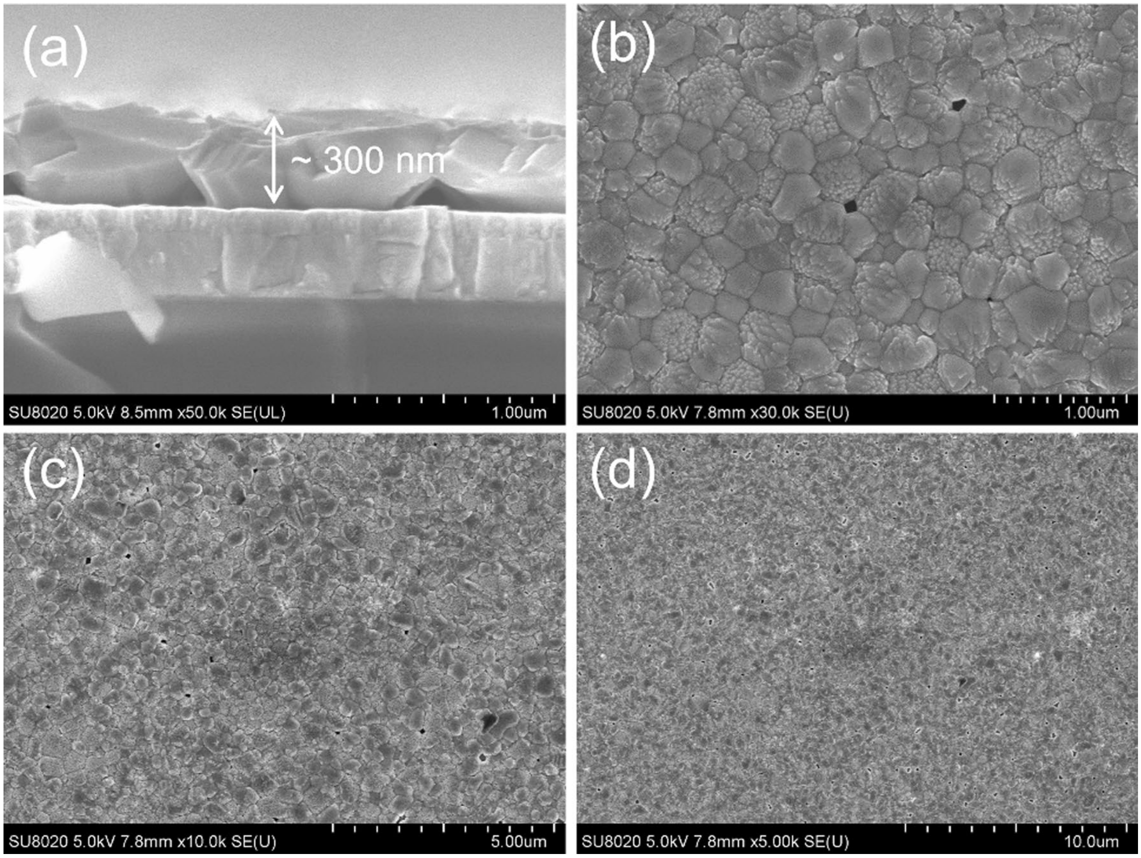

Fig. 4 SEM images of $BiVO_4$. **a** The cross-sectional view of $BiVO_4$. **b**–**d** The top view of $BiVO_4$

Experimental

Anodic-plating of $Bi_4O_4(OH)_2CO_3$ film on ITO glass

A 0.1 M $Bi(NO_3)_3$ solution was prepared by dissolving $Bi(NO_3)_3 \cdot 5H_2O$ in 25 ml acetic acid solution (99.7% mass ratio, Wako). The prepared solution was mixed with a 10 mL pH 5 sodium acetate aqueous solution. 5 M NaOH solution was used to adjust the pH of the mixed solution to 4.8. Anodic plating was performed at 2.3 $V_{Ag/AgCl}$ at room temperature using a three-electrode cell with ITO working electrodes, a platinum counter electrode and an Ag/AgCl reference electrode. A potentiostat (CHI630e) was used for anodic plating and subsequent electrochemical measurements. The optimum plating time was 7 min.

Fabrication of $BiVO_4$ thin film on ITO glass

First, ~ 300 nm amorphous $Bi_4O_4(OH)_2CO_3$ film was anodically plated on an ITO glass in a bismuth nitrite and sodium acetate aqueous solution. Drop-casting vanadyl acetylacetonate ($VO(acac)_2$) organic solutions onto the plated $Bi_4O_4(OH)_2CO_3$ films allowed homogeneous mix of the V and Bi species. The mixed samples were annealed at different temperatures. Finally, the obtained film samples were washed with NaOH to remove impurities. In detail, 0.075 mL 0.2 M $VO(acac)_2$ dimethyl sulfoxide solution was dropped on the $Bi_4O_4(OH)_2CO_3$ films (2 cm × 2 cm) and then calcined in a furnace at 520 °C for 2 h in air. Remained VO_x on top of the $BiVO_4$ films was washed in 1 M NaOH solution for 10 min with gentle stirring.

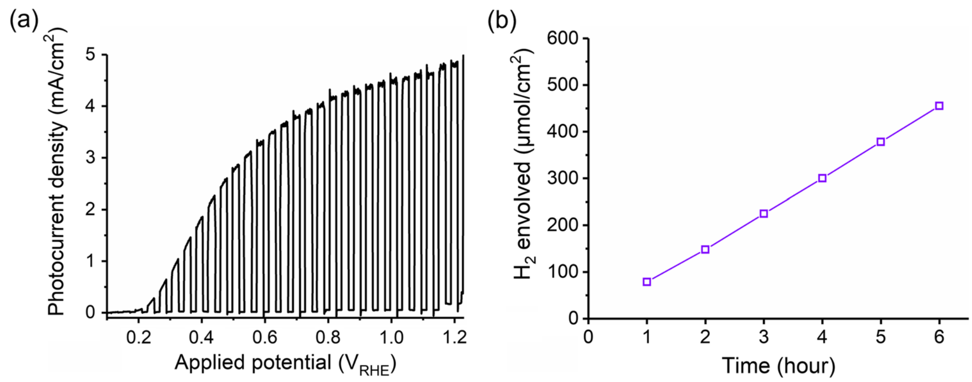

Fig. 5 Photoelectrochemical performance of $BiVO_4$ film in a 0.1 M potassium phosphate (KPi) and 0.1 M Na_2SO_3 solution. **a** Photocurrent densities at 0–1.2 V_{RHE}; **b** evolved H_2 in 6 h

Measurements

The scanning electron microscopic (SEM) images were obtained by a Hitachi SU8020. The XRD diffraction spectra were performed using the smart lab XRD of Rigaku, Japan. The XPS analyses were performed using Mg Kα (1253.6 eV) photon energy. During XPS depth profile studies, Ar bombardment with an etching speed of several tens nm/time was used. Binding energy peak shifts due to any charging were normalized with C 1s peak set to 284.8 eV and Fermi energy position. The TGA analyses were conducted with a differential thermogravimetric analyzer (Rigaku, Japan). The PEC performances were measured by a three-electrode electrochemical configuration with a 0.1 M Na_2SO_3 solution under simulated sunlight illumination (SAN-EI electronic, XES40S1, AM 1.5G, 100 mW cm^{-2}). An Ag/AgCl electrode was used as a reference electrode, and a Pt coil was used as a counter electrode. The measured potentials were all converted to the reversible hydrogen electrode according to the Nernst equation:

$$V_{\mathrm{RHE}} = V_{\mathrm{Ag/AgCl}} + 0.059\,\mathrm{pH} + V^{0}_{\mathrm{Ag/AgCl}} \quad (2)$$

$$V^{0}_{\mathrm{Ag/AgCl}} = 0.199\,\mathrm{V\ at\ 25\ ^{\circ}C} \quad (3)$$

The PEC cell was connected to a vacuum pump and a micro-GC (Agilent 990 micro). Before measurement, the PEC cell was pumped to a low vacuum, and Ar gas was used to purge out the N_2 and O_2 gases in the cell. The H_2 evolution was measured in under simulated sunlight illumination for 6 h at 0.9 V_{RHE}. The theoretical amounts of evolved H_2 were estimated from the passed charges on the assumption that faradaic efficiency was unity.

Acknowledgements The authors acknowledge Prof. Kazunari Domen and his group for assistance in the material fabrication and characterization.

Author contributions M.Z. supervised the project. M.Z. and H.J. conceived the idea and designed the experiments. H.J. performed the synthesis, characterizations, and performance tests. M.Z., H.J. and Y.X. wrote the manuscript. All authors discussed the results and assisted during manuscript preparation.

Funding This work was supported by the National Key Research and Development Program of the Ministry of Science and Technology of China (No. 2020YFA0406102), the National Natural Science Foundation of China (Grant Number 22272078, 91963121), and the Frontiers Science Center for Critical Earth Material Cycling of Nanjing University, "Innovation & Enterpreneurship Talents" plan of Jiangsu Province.

Data availability The datasets used and/or analyzed during the current study are available from the corresponding author on reasonable request.

Declarations

Ethics approval and consent to participate Not applicable.

Consent for publication Not applicable.

Competing interests The authors declare no competing interests.

References

1. Grätzel M. Photoelectrochemical cells. Nature. 2001;414:338–44. https://doi.org/10.1038/35104607.
2. Reece SY, Hamel JA, Sung K, et al. Wireless solar water splitting using silicon-based semiconductors and earth-abundant catalysts. Science. 2011;334:645–8. https://doi.org/10.1126/science.1209816.
3. Wang Q, Hisatomi T, Ma SSK, et al. Core/shell structured La- and Rh-codoped SrTiO3 as a hydrogen evolution photocatalyst in Z-scheme overall water splitting under visible light irradiation. Chem Mater. 2014;26:4144–50. https://doi.org/10.1021/cm5011983.
4. Zhong M, Tran K, Min Y, et al. Accelerated discovery of CO 2 electrocatalysts using active machine learning. Nature. 2020;581:178–83. https://doi.org/10.1038/s41586-020-2242-8.
5. Li L, Ozden A, Guo S, et al. Stable, active CO2 reduction to formate via redox-modulated stabilization of active sites. Nat Commun. 2021;12:5223. https://doi.org/10.1038/s41467-021-25573-9.
6. Jin L, Zhao H, Wang ZM, Rosei F. Quantum dots-based photoelectrochemical hydrogen evolution from water splitting. Adv Energy Mater. 2021;11:2003233. https://doi.org/10.1002/aenm.202003233.
7. Jiang C, Moniz SJA, Wang A, et al. Photoelectrochemical devices for solar water splitting—materials and challenges. Chem Soc Rev. 2017;46:4645–60. https://doi.org/10.1039/C6CS00306K.
8. Zhong M, Hisatomi T, Minegishi T, et al. Bulky crystalline BiVO4 thin films for efficient solar water splitting. J Mater Chem A. 2016;4:9858–64. https://doi.org/10.1039/C6TA03072F.
9. Zhong M, Hisatomi T, Kuang Y, et al. Surface modification of CoOx loaded BiVO4 photoanodes with ultrathin p-Type NiO layers for improved solar water oxidation. J Am Chem Soc. 2015;137:5053–60. https://doi.org/10.1021/jacs.5b00256.
10. Sivula K, van de Krol R. Semiconducting materials for photoelectrochemical energy conversion. Nat Rev Mater. 2016;1:1–16. https://doi.org/10.1038/natrevmats.2015.10.
11. Andrei V, Jagt RA, Rahaman M, et al. Long-term solar water and CO2 splitting with photoelectrochemical BiOI–BiVO4 tandems. Nat Mater. 2022;21:864–8. https://doi.org/10.1038/s41563-022-01262-w.
12. Abdi FF, Han L, Smets AHM, et al. Efficient solar water splitting by enhanced charge separation in a bismuth vanadate-silicon tandem photoelectrode. Nat Commun. 2013;4:2195. https://doi.org/10.1038/ncomms3195.
13. Seabold JA, Choi K-S. Efficient and stable photo-oxidation of water by a bismuth vanadate photoanode coupled with an iron oxyhydroxide oxygen evolution catalyst. J Am Chem Soc. 2012;134:2186–92. https://doi.org/10.1021/ja209001d.
14. Kuang Y, Yamada T, Domen K. Surface and interface engineering for photoelectrochemical water oxidation. Joule. 2017;1:290–305. https://doi.org/10.1016/j.joule.2017.08.004.
15. Kim TW, Choi K-S. Nanoporous BiVO4 photoanodes with dual-layer oxygen evolution catalysts for solar water splitting. Science. 2014;343:990–4. https://doi.org/10.1126/science.1246913.
16. Frondel C. Mineralogy of the calcium phosphates in insular phosphate rock. Am Miner. 1943;28:215–32.
17. Taylor P, Sunder S, Lopata VJ. Structure, spectra, and stability of solid bismuth carbonates. Can J Chem. 1984;62:2863–73. https://doi.org/10.1139/v84-484.
18. Dong F, Zheng A, Sun Y, et al. One-pot template-free synthesis, growth mechanism and enhanced photocatalytic activity of monodisperse (BiO)2CO3 hierarchical hollow microspheres self-assembled with single-crystalline nanosheets. CrystEngComm. 2012;14:3534–44. https://doi.org/10.1039/C2CE06677G.